

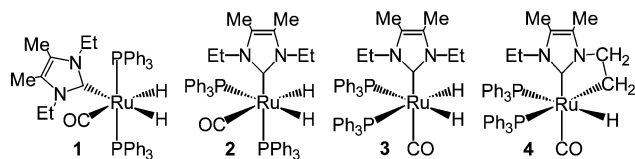
## Photochemical Isomerization of N-Heterocyclic Carbene Ruthenium Hydride Complexes: In situ Photolysis, Parahydrogen, and Computational Studies

Kirsten A. M. Ampt,<sup>‡</sup> Suzanne Burling,<sup>†</sup> Steven M. A. Donald,<sup>§</sup> Susie Douglas,<sup>†</sup> Simon B. Duckett,<sup>\*,‡</sup> Stuart A. Macgregor,<sup>\*,§</sup> Robin N. Perutz,<sup>‡</sup> and Michael K. Whittlesey<sup>\*,†</sup>

*Department of Chemistry, University of York, Heslington, York YO10 5DD, U.K., Department of Chemistry, University of Bath, Claverton Down, Bath BA2 7AY, U.K., and School of Engineering and Physical Sciences, Heriot-Watt University, Edinburgh, EH14 4AS, U.K.*

Received April 2, 2006; E-mail: chsmkw@bath.ac.uk

Over the past decade, N-heterocyclic carbenes (NHCs) have become an important class of ligands as alternatives to phosphines in inorganic chemistry.<sup>1</sup> Their strong  $\sigma$ -donor properties have been used to successfully manipulate the stability and reactivity of catalytically important metal fragments.<sup>2</sup> It seems remarkable, however, that their effect on the chemistry of photochemically formed coordinatively unsaturated metal species has yet to be studied. In this communication, we describe how UV irradiation of the NHC-containing dihydride complex  $\text{Ru}(\text{IEt}_2\text{Me}_2)(\text{PPh}_3)_2(\text{CO})\text{H}_2$  (**1**,  $\text{IEt}_2\text{Me}_2 = 1,3$ -bis(ethyl)-4,5-dimethylimidazol-2-ylidene)<sup>3</sup> results in a very facile isomerization reaction involving loss of either  $\text{H}_2$  or phosphine. This contrasts the reported photochemistry of the all-phosphine species  $\text{Ru}(\text{PPh}_3)_3(\text{CO})\text{H}_2$ , which loses only  $\text{H}_2$  on the way to postulated dimeric products.<sup>4</sup> We describe the use of a unique combination of in situ photolysis with NMR detection, parahydrogen, and DFT calculations to map both intermediates and photoproducts in the reactions of **1**.



Irradiation of a  $d_8$ -toluene sample of **1** at  $<223$  K (Hg arc, 125 W, 6 h), followed by rapid transfer into the NMR spectrometer for observation at 223 K, revealed the partial isomerization of **1** into **2**, which displays hydride resonances in the low-temperature  $^1\text{H}$  NMR spectrum at  $\delta -5.6$  and  $-7.3$  (each with ddd multiplicity) and two mutually coupled doublets in the  $^{31}\text{P}\{^1\text{H}\}$  NMR spectrum. Upon warming, **2** cleanly reforms **1**. To elucidate the pathway for photoisomerization in more detail, a second sample of **1** was subjected to in situ photolysis (325 nm HeCd laser, 38 mW) within the NMR probe at 223 K. After 120 s of irradiation, 7% of **1** converts into a 1:1 mixture of **2** and a new isomer **3**. The  $^1\text{H}\{^{31}\text{P}\}$  NMR spectrum displays the expected two hydride doublets for **2** and a singlet for **3** ( $\delta -7.0$ ; couples to a single  $^{31}\text{P}$  resonance at  $\delta 43.9$ ). Upon further photolysis, the ratio of **2**:**3** changes to favor **2**, and signals for the C–H activated species **4** were also observed to grow in ( $^1\text{H}$ :  $\delta -7.1$ , dd,  $J_{\text{HP}} = 102.6$ ,  $J_{\text{HP}} = 25.8$  Hz;  $^{31}\text{P}\{^1\text{H}\}$ :  $\delta 56.9$ , d, 36.6 d,  $J_{\text{PP}} = 18.0$  Hz).<sup>5</sup>

The time course plot showing the experimentally observed variation in proportions of **1**, **2**, **3**, and **4** with photolysis time is shown in Figure 1. The trace was simulated for a series of first-order interconversion processes to yield an empirical understanding

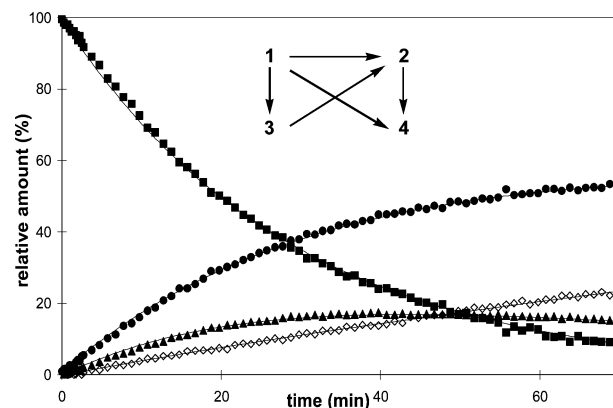


**Figure 1.** Time profile for conversion of **1** (■) into **2** (●), **3** (▲), and **4** (◇) over 70 min upon photolysis at 223 K (observed points and fitted lines with the dominant pathways indicated).

of the available pathways. This procedure revealed that (i) **1** converts readily into both **2** (rate constants reported relative to  $k_{12} = 1.00$  (reciprocal time)) and **3** ( $k_{13} = 0.57$ ), (ii) **4** forms from both **1** and **2** ( $k_{14} \approx k_{24} = 0.23$ ), (iii) **2** and **3** have lower photochemical activity than **1**, (iv) **3** converts to **2** photochemically, and (v) **4** is stable under photolysis at 223 K.

To examine the individual steps involved in these transformations, **1** was irradiated (223 K) in  $d_8$ -toluene under 3 atm of  $p\text{-H}_2$ . Enhanced hydride resonances for both **2** and **3** were immediately apparent in the corresponding  $^1\text{H}$  NMR spectrum (Figure 2a); with  $^{31}\text{P}$  decoupling (Figure 2b), the two hydride resonances observed for **1** match expectations for unenhanced doublets superimposed on weak antiphase doublets. This observation indicates that the hydride ligands of **1** are partially exchanged for those of  $p\text{-H}_2$ . One of the pathways for the isomerization of **1** to **2** and **3**, therefore, must involve the photochemical loss of  $\text{H}_2$  to give the 16e fragment  $\text{Ru}(\text{IEt}_2\text{Me}_2)(\text{PPh}_3)_2(\text{CO})$ . DFT calculations<sup>6</sup> on the full species **1**, **2**, and **3** predict the relative stabilities  $\mathbf{1} \approx \mathbf{2} > \mathbf{3}$  (Figure 3), so in conjunction with the fact that **2** reforms **1** thermally, we conclude that the photolysis reaction is under kinetic control. These calculations located two forms of  $\text{Ru}(\text{IEt}_2\text{Me}_2)(\text{PPh}_3)_2(\text{CO})$ , **A** and **B**. Their reaction with  $\text{H}_2$  leads directly to **3** and **2**, respectively, but **4** could only be formed from intermediate **A**. The selectivity for  $\text{H}_2$  addition to **A** and **B** can be estimated from the  $p\text{-H}_2$  data, which show a 1:3.7 ratio for the  $p\text{-H}_2$  enhanced hydride signals for **1** and **2**.<sup>7</sup>

The roles of different quenching agents on the isomer distribution formed upon in situ photolysis conditions have also been assessed.  $^1\text{H}\{^{31}\text{P}\}$  NMR spectra obtained after 50% conversion in the presence or absence of  $\text{H}_2$  showed no difference in the relative amounts of **1**, **2**, and **3**, indicating that  $\text{H}_2$  does not reduce the rate of isomerization of **1** into **2** and **3**.<sup>8</sup> Evidence for a photochemical

<sup>‡</sup> University of York.

<sup>†</sup> University of Bath.

<sup>§</sup> Heriot-Watt University.

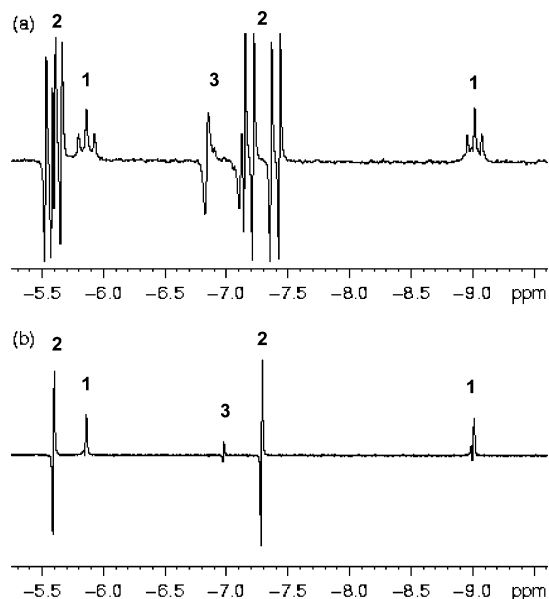


**Figure 2.**  $^1\text{H}$  NMR spectra showing the hydride region only of  $d_8$ -toluene solutions of **1** under UV photolysis with  $p\text{-H}_2$  at 223 K. (a) Fully coupled spectrum, with enhanced resonances for **2** and **3** indicated. (b)  $^1\text{H}\{^{31}\text{P}\}$  spectrum showing weak signal enhancement for **1**.

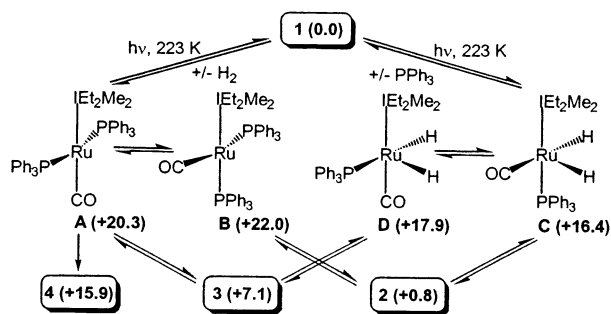


**Figure 3.** Computed reaction profile (kcal/mol) for the interconversions of **1**, **2**, **3**, and **4** via  $\text{H}_2$  and  $\text{PPh}_3$  loss pathways.

process involving  $\text{PPh}_3$  loss<sup>9</sup> was obtained at extended irradiation times under  $\text{H}_2$  at 223 K. This gave rise to two very broad hydride resonances ( $\delta$   $-5.4$  and  $-4.9$ ), with measured  $T_1$  values of ca. 15 and 22 ms, respectively, that are consistent with an  $\eta^2\text{-H}_2$  complex.<sup>10</sup> These signals disappeared very quickly upon warming to 223 K; when the photolysis of **1** was performed in the presence of both  $\text{PPh}_3$  and  $\text{H}_2$ , the formation of this species was suppressed. We therefore conclude that this species is the phosphine loss product  $\text{Ru}(\text{IEt}_2\text{Me}_2)(\text{PPh}_3)(\text{CO})(\eta^2\text{-H}_2)\text{H}_2$ , **6**.<sup>11</sup> Confirmation of a phosphine loss pathway was obtained by in situ irradiation of **1** in  $d_8$ -toluene in the presence of an 8.6-fold excess of pyridine. This led to the immediate formation of a new monophosphine dihydride species, which we assign as  $\text{Ru}(\text{IEt}_2\text{Me}_2)(\text{PPh}_3)(\text{C}_5\text{H}_5\text{N})(\text{CO})\text{H}_2$ , **7** ( $^1\text{H}$  NMR:  $\delta$   $-3.3$ , dd,  $J_{\text{HH}} = -9.0$  Hz,  $J_{\text{HP}} = 31.5$  Hz;  $\delta$   $-14.2$ , dd,  $J_{\text{HH}} = -9.0$ ,  $J_{\text{HP}} = 21.0$  Hz), with hydride ligands *trans* to CO and pyridine, respectively, by comparison to the NMR of the related species  $\text{Ru}(\text{PR}_3)(\text{C}_5\text{H}_5\text{N})(\text{CO})_2\text{H}_2$ .<sup>12</sup> In spectra recorded at early reaction times, the formation of both **2** and **3** was essentially

quenched. This suggests that **1** undergoes photochemical phosphine loss as the dominant reaction pathway, leading to **7** via trapping of the same 16e intermediate that leads to **2**.

Computed energies for likely intermediates on a phosphine loss pathway are included in Figure 3. The calculations show that  $\text{PPh}_3$  loss from **1** is accompanied by spontaneous isomerization of the resultant five-coordinate species<sup>13</sup> to form isomer **C**. This isomer can then add  $\text{PPh}_3$  directly to form **2** or isomerize to **D** with  $\text{PPh}_3$  addition then yielding **3**. Once **C** is formed, there is therefore no direct low-energy pathway back to **1**. Experimental confirmation of this was seen upon photolysis of **1** in the presence of a 50-fold excess of  $\text{PPh}_3$ , which showed the production of **2** and **3** to be essentially unaffected. This is consistent with the formation of **2** and **3** upon photolysis being independent of phosphine concentration, assuming the **C**–**D** isomerization is rapid.

In summary, we have shown that incorporation of an N-heterocyclic carbene into  $\text{Ru}(\text{PPh}_3)_3(\text{CO})\text{H}_2$  has a dramatic effect on the overall photochemistry. The observed photoisomerization reaction involves loss of both  $\text{H}_2$  and  $\text{PPh}_3$ , as revealed by a combination of in situ photolysis/ $p\text{-H}_2$  studies allied with DFT calculations. This combination of approaches has also provided a unique insight into the role that key 16e intermediates play in these processes. In light of the high reactivity associated with photochemically generated M- $\text{PR}_3$  fragments in activating C–H bonds,<sup>14</sup> studies of their NHC analogues certainly warrant future investigations.

**Acknowledgment.** We thank the EPSRC for support.

**Supporting Information Available:** Kinetic and computational data. Complete ref 6. This material is available free of charge via the Internet at <http://pubs.acs.org>.

## References

- Scott, N. M.; Nolan, S. P. *Eur. J. Inorg. Chem.* **2005**, *10*, 1815.
- Grubbs, R. H. *Tetrahedron* **2004**, *60*, 7117.
- Burling, S.; Mahon, M. F.; Paine, M. F.; Whittlesey, M. K.; Williams, J. M. J. *Organometallics* **2004**, *23*, 4537.
- (a) Geoffroy, G. L.; Bradley, M. G. *Inorg. Chem.* **1977**, *16*, 744. (b) Colombo, M.; George, M. W.; Moore, J. N.; Pattison, D. I.; Perutz, R. N.; Virrels, I. G.; Ye, T.-Q. *J. Chem. Soc., Dalton Trans.* **1997**, 2857.
- A different isomer of this C–H activated complex is reported in ref 3.
- Frisch, M.; et al.; *Gaussian 98*, revision A.11.4; Gaussian, Inc.: Pittsburgh, PA, 2001. Calculations used the BP86 functional. Ru and P were described with Stuttgart RECPs and associated basis sets. 6-31G\*\* basis sets were used for all other atoms, with the exception of phosphine groups, where 6-31G was employed. Energies include corrections for zero-point energy. See Supporting Information for details.
- Since enhancement of the hydride signals in **3** results from their origin in a second-order spin system, its proportion cannot be estimated.
- The formation of **4**, however, was suppressed by  $\text{H}_2$ .
- (a) Bruno, J. W.; Huffman, J. C.; Green, M. A.; Zubkowski, J. D.; Hatfield, W. E.; Caulton, K. G. *Organometallics* **1990**, *9*, 2556. (b) Montiel-Palma, V.; Perutz, R. N.; George, M. W.; Jina, O. S.; Sabo-Etienne, S. *Chem. Commun.* **2000**, 1175.
- The broadness of the hydride and  $\eta^2$ -dihydrogen signals is consistent with exchange as seen in closely related complexes. See: Giunta, K. D.; Hölscher, M.; Lehmann, C. W.; Mynott, R.; Wirtz, C.; Leitner, W. *Adv. Synth. Catal.* **2003**, *345*, 1139.
- It is at the point where the detection of **6** is possible that the PHIP effect is no longer visible. This suggests that rapid exchange of the  $\eta^2\text{-H}_2$  ligand with free  $p\text{-H}_2$  leads to the destruction of  $p\text{-H}_2$  enhancement.
- Dunne, J. P.; Blazina, D.; Aiken, S.; Carteret, H. A.; Duckett, S. B.; Jones, J. A.; Poli, R.; Whitwood, A. C. *Dalton Trans.* **2004**, 3616.
- The calculated energy of the  $\{\text{Ru}(\text{IEt}_2\text{Me}_2)(\text{PPh}_3)(\text{CO})\text{H}_2\}$  fragment formed upon  $\text{PPh}_3$  loss from **1** is +34 kcal/mol.
- Baker, M. V.; Field, L. D. *J. Am. Chem. Soc.* **1987**, *109*, 2825.

JA0622397